

# Multiresolution quantum field theory in light-front coordinates

Mikhail V. Altaisky,<sup>1</sup> Natalia E. Kaputkina,<sup>2</sup> and Robin Raj<sup>3</sup>

<sup>1)</sup>*Space Research Institute RAS, Profsoyuznaya 84/32, Moscow, 117997, Russia<sup>a)</sup>*

<sup>2)</sup>*National University of Science and Technology 'MISIS', Leninsky av. 4, Moscow, 119049, Russia<sup>b)</sup>*

<sup>3)</sup>*Mahatma Gandhi University, Priyadarsini Hills, Kottayam, Kerala, 686560, India<sup>c)</sup>*

(Dated: Feb 11, 2022)

We analyse the use of wavelet transform in quantum field theory models written in light-front coordinates. In a recent paper<sup>1</sup> W.N.Polyzou used  $x^+$  variable as 'time', and applied wavelet transform to the 'spatial' coordinates only. This makes the theory asymmetric with respect to space and time coordinates. In present paper we generalise the concept of continuous causal path, which is the basis of path integration, to the sequences of causally ordered spacetime regions, and present evaluation rules for Feynman path integrals over such sequences in terms of wavelet transform. Both the path integrals and the wavelet transform in our model are symmetric with respect to the light-front variables  $(x^+, x^-)$ . The definition of a spacetime event in our generalization is very much like the definition of event in probability theory.

Keywords: Quantum field theory, regularisation, causality, wavelets

---

<sup>a)</sup>Electronic mail: altaisky@rssi.ru

<sup>b)</sup>Electronic mail: kaputkina.ne@misis.ru

<sup>c)</sup>Electronic mail: robuka97@gmail.com

## I. INTRODUCTION

The Feynman path integral is the basic tool of quantum field theory (QFT) and statistical mechanics. Having initially originated from the Dirac idea that the transition of a quantum system from initial state  $q_i$  at the time instant  $t_i$  to the final state  $q_f$  at the time  $t_f$  can be represented by the integral over all possible intermediate states  $q_\tau, t_i < \tau < t_f$ , of the exponent of the Lagrangian  $\exp\left(\frac{i}{\hbar} \int_{t_i}^{t_f} L[q(\tau)] d\tau\right)^2$ . Feynman has successfully applied the Dirac method to generate a self-consistent Lorentz-invariant perturbation theory in quantum electrodynamics (QED) from an infinite-dimensional integral over all possible field configurations in Minkowski space<sup>3</sup>.

Green functions calculated by the Feynman expansion suffer from divergences and cannot be compared to experimental results, unless a special procedure, called *renormalization* is applied to get rid of UV divergences. A way of getting tractable results without renormalization has been proposed in a series of papers<sup>4-6</sup>. It consists in changing the functional space of local square-integrable fields  $\phi = \phi(x)$  to the space of functions that depend on both the spacetime point ( $x$ ) and the size of the region ( $a$ ) the measurement can be made on:  $\phi = \phi_a(x)$ . For a local field an attempt to measure some physical quantity sharp at a point  $x$ , i.e., at  $\Delta x \rightarrow 0$ , demands an infinite momentum transfer  $\Delta p \sim \frac{\hbar}{\Delta x} \rightarrow \infty$ , which drives the theory out of its applicability domain by means of UV divergences. For a scale-dependent field  $\phi_a(x)$  no such problem exists because the observation scale  $a$  always remains finite. The dependence on the observation scale is given by the logarithmic derivatives  $a \frac{\partial}{\partial a}$  that describe the renormalization of parameters of the scale-dependent quantum field theory<sup>7</sup>.

To define the path integral in terms of the fields that can be observed over a finite-size regions, we first need to define *what are these paths*. In standard approach, Feynman path is a causally-ordered continuous set of points of the Minkowski space, with each point  $(t, \mathbf{x})$  considered as a label of a potential event, such as particle creation, or particle annihilation. This definition, adopted in local quantum field theory, has no respect to the *finiteness* of the spacetime region, where something can be measured. To define the path integral in terms of the potentially measured quantities we need something similar to the  $\sigma$ -algebra of events adopted in probability theory<sup>8</sup>. At the same time the construction should be invariant under the Lorentz transformations, providing the speed of light is the same in any inertial frame of reference.

In the present paper we make an endeavour to define the causal paths in the space of events using the light-front coordinates in Minkowski space and a set of basic functions which provide the construction of wavelet transform in light-front variables. Our model is essentially different from usual construction of path integral in terms of the light-front variables, where the  $x^+$  variable is used as a 'time', which orders the events, with the  $x^-$  variables being considered as a 'spatial' coordinate<sup>9</sup>. The path integral, which describes the transition amplitude from the initial field configuration defined on a spacetime region  $A$  to the final field configuration defined on a spacetime region  $B$ , so that  $B$  is inside the forward light-cone of  $A$ , is completely symmetric with respect to the  $x^+$  and the  $x^-$  variables, and hence is symmetric with respect to space and time in any Lorentzian frame of reference.

The remainder of this paper is organized as follows. In *Section II* we remind the introduction of scale-dependent functions by means of wavelet transform. *Section III* presents an example of a finite Euclidean quantum field theory model with  $\phi^4$  interaction using continuous wavelet transform. In *Section IV* we present a construction of the generating functional of scale-dependent Green functions by means of discrete wavelet transform on a finite domain  $[0, T] \otimes [0, T]$  in light-front coordinates  $(x^+, x^-)$ . The analysis of the causality aspects of the presented wavelet-based construction ensures it is symmetric with respect to space and time variables. The path integration is performed over the sequences of causally connected events of finite size. The virtues and the problems of our approach are summarized in *Conclusion*.

## II. SCALE-DEPENDENT FUNCTIONS

### A. Wavelet transform in $L^2(\mathbb{R})$

The idea of substituting a local field  $\phi(x)$ ,  $x \in \mathbb{R}^d$  by a collection of local fields  $\{\phi_a(x)\}_a$ ,  $a \in \mathbb{R}_+$  has first emerged in geophysics<sup>10</sup>, where *non-local* separation of different components of the seismic signal by means of Fourier transform

$$\phi(x) \xrightarrow{\mathcal{F}} \tilde{\phi}(k)$$

failed to provide reliable separation of localized signals with similar content of Fourier harmonics. An alternative to Fourier transform was found in the convolution of the analysed signal  $\phi(x)$  with certain well-localized function  $\chi(x)$ , usually referred to as a *mother wavelet*,

shifted by  $b$  and dilated by  $a$ :

$$\phi_a(b) := \int_{\mathbb{R}} \frac{1}{a} \bar{\chi} \left( \frac{x-b}{a} \right) \phi(x) dx. \quad (1)$$

The functions  $\phi_a(b)$  are called *wavelet coefficients* of the square-integrable function  $\phi(x)$  with respect to the mother wavelet  $\chi(x)$ . (Following<sup>5,11</sup> we have changed the  $L^2(\mathbb{R})$  normalisation  $\frac{1}{\sqrt{a}}\chi\left(\frac{x-b}{a}\right)$  to the  $L^1$  normalisation to make wavelet coefficients the same physical dimension as that of the original fields.) The function  $\phi(x)$  can be reconstructed from the set of its wavelet coefficients by means of *inverse wavelet transform*:

$$\phi(x) = \frac{1}{C_\chi} \int_{\mathbb{R}_+ \otimes \mathbb{R}} \frac{1}{a} \chi \left( \frac{x-b}{a} \right) \phi_a(b) \frac{dad b}{a}. \quad (2)$$

The admissibility condition for the basic wavelet  $\chi$  is rather loose: only the finiteness

$$C_\chi = \int_0^\infty |\tilde{\chi}(a)|^2 \frac{da}{a} < \infty, \quad \text{where } \tilde{\chi}(k) := \int_{-\infty}^\infty e^{ikx} \chi(x) dx, \quad (3)$$

is required to ensure the wavelet transform is invertible.

The convolutions (1) and (2) have clear physical interpretations: applying a 'microscope' with an aperture function  $\chi(x)$  we scrutinize the function  $\phi$  locally at all possible resolutions; the convolution (2) reconstructs function  $\phi$  from a set of its components of all scales<sup>12</sup>. Wavelet transform, as a separation of a function into a set of its scale components, can be written in both the continuous form, Eq.(1,2), and the discrete form<sup>13</sup>.

## B. Continuous wavelet transform

Wavelet transform is a natural generalization of the Fourier transform for the case when the *scaling* properties of the theory are important. Let  $\mathcal{H}$  be a Hilbert space of states of quantum field  $|\phi\rangle$ . Let  $|x\rangle \in \mathcal{H}$  be a vector corresponding to the localization at point  $x$ , then

$$\phi(x) = \langle x | \phi \rangle \quad (4)$$

is a coordinate representation of the field  $|\phi\rangle$ . The Fourier transform is the decomposition of the field  $|\phi\rangle$  with respect to the representations of the translation group:

$$\langle x | \phi \rangle = \int \langle x | p \rangle dp \langle p | \phi \rangle,$$

where  $|p\rangle$  is an eigenvector of the translation operator.

Similarly, let  $G$  be a locally compact Lie group acting transitively on  $\mathcal{H}$ , with  $d\mu(\nu), \nu \in G$  being a left-invariant measure on  $G$ , then, any  $|\phi\rangle \in \mathcal{H}$  can be decomposed with respect to a representation  $\Omega(\nu)$  of  $G$  in  $\mathcal{H}^{14,15}$ :

$$|\phi\rangle = \frac{1}{C_\chi} \int_G \Omega(\nu) |\chi\rangle d\mu(\nu) \langle \chi | \Omega^\dagger(\nu) | \phi \rangle, \quad (5)$$

where  $|\chi\rangle \in \mathcal{H}$  is a 'mother wavelet', or an admissible vector, satisfying the admissibility condition

$$C_\chi = \frac{1}{\|\chi\|^2} \int_G |\langle \chi | \Omega(\nu) | \chi \rangle|^2 d\mu(\nu) < \infty.$$

The coefficients  $\langle \chi | \Omega^\dagger(\nu) | \phi \rangle$  are known as wavelet coefficients in a general sense.

If the group  $G$  is Abelian, the wavelet transform (5) with  $G : x' = x + b'$  is the Fourier transform. The next to the Abelian group is the group of the affine transformations of the Euclidean space  $\mathbb{R}^d$ :

$$G : x' = aR(\theta)x + b, \quad x, b \in \mathbb{R}^d, a \in \mathbb{R}_+, \quad (6)$$

where  $R(\theta)$  is the  $SO(d)$  rotation matrix. Here we define the representation of the affine transform (6) with respect to the mother wavelet  $\chi(x)$  as follows:

$$\Omega(a, b, \theta) \chi(x) = \frac{1}{a^d} \chi \left( R^{-1}(\theta) \frac{x - b}{a} \right). \quad (7)$$

Thus the wavelet coefficients of the function  $\phi(x) \in L^2(\mathbb{R}^d)$  with respect to the mother wavelet  $\chi(x)$  in Euclidean space  $\mathbb{R}^d$  can be written as

$$\phi_{a,\theta}(b) = \int_{\mathbb{R}^d} \frac{1}{a^d} \overline{\chi \left( R^{-1}(\theta) \frac{x - b}{a} \right)} \phi(x) d^d x. \quad (8)$$

The function  $\phi(x)$  can be reconstructed from its wavelet coefficients (8) using the formula (5):

$$\phi(x) = \frac{1}{C_\chi} \int \frac{1}{a^d} \chi \left( R^{-1}(\theta) \frac{x - b}{a} \right) \phi_{a,\theta}(b) \frac{da db}{a} d\mu(\theta), \quad (9)$$

where  $d\mu(\theta)$  is the left-invariant measure on the  $SO(d)$  rotation group, usually written in terms of the Euler angles:

$$d\mu(\theta) = 2\pi \prod_{k=1}^{d-2} \int_0^\pi \sin^k \theta_k d\theta_k.$$

The normalization constant  $C_\chi$  is readily evaluated using Fourier transform. For isotropic wavelets

$$C_\chi = \int_0^\infty |\tilde{\chi}(ak)|^2 \frac{da}{a} = \int |\tilde{\chi}(k)|^2 \frac{d^d k}{S_d |k|^d} < \infty, \quad (10)$$

where  $S_d = \frac{2\pi^{d/2}}{\Gamma(d/2)}$  is the area of unit sphere in  $\mathbb{R}^d$ , with  $\Gamma(x)$  being the Euler's Gamma function. Tilde means the Fourier transform:  $\tilde{\chi}(k) = \int_{\mathbb{R}^d} e^{ikx} \chi(x) d^d x$ .

### C. Discrete wavelet transform

The convolution of continuous and differentiable mother wavelet, shifted and dilated, with the analysed function is not very efficient numerically. For practical analysis, thanks to the works of I.Daubechies and other authors, we often use the frames of orthogonal wavelets, which provides fast and efficient data processing<sup>16</sup>. Let us briefly remind the basics of the discrete wavelet transform<sup>13,17</sup>.

The implementation of the discrete version of wavelet transform is intimately related to the *Mallat multiresolution analysis* (MRA)<sup>18</sup>. Having been used in signal processing for quite some time before wavelets, the multiresolution analysis in the Hilbert space of square-integrable functions  $L^2(\mathbb{R})$ , or

**Definition 1** *The Mallat sequence, is an increasing sequence of closed subspaces  $\{V_j\}_{j \in \mathbb{Z}}$ ,  $V_j \in L^2(\mathbb{R})$ , such that*

1.  $\dots \subset V_0 \subset V_1 \subset V_2 \subset \dots \subset L^2(\mathbb{R})$
2.  $\text{clos}_{L^2} \cup_{j \in \mathbb{Z}} V_j = L^2(\mathbb{R})$
3.  $\cap_{j \in \mathbb{Z}} V_j = \emptyset$
4. *The spaces  $V_j$  and  $V_{j+1}$  are "similar" in a sense that*

$$f(x) \in V_j \Leftrightarrow f(2x) \in V_{j+1}, \quad j \in \mathbb{Z}.$$

The property 4) is a key feature of the MRA sequence: If a set of functions  $\varphi_k^0 \equiv \varphi(x - k)$  forms a Riesz basis in  $V_0$ , it automatically implies that the set

$$\varphi_k^j = 2^{\frac{j}{2}} \varphi(2^j x - k)$$

forms a basis in  $V_j$ . Due to the inclusion property 1), any function  $f(x) \in V_0$  can be written as a sum of basic functions from  $V_1$ :

$$f(x) = \sum_k c_k 2^{\frac{1}{2}} \varphi(2x - k).$$

For this reason

$$V_1 = V_0 \oplus W_0,$$

which is the definition of the orthogonal complement of  $V_0$  to  $V_1$ . Similarly,

$$V_2 = V_1 \oplus W_1, \quad V_2 = V_0 \oplus W_0 \oplus W_1,$$

and so on.

The basic functions  $\varphi_k^j$  in  $V_j$  spaces are usually referred to as the *scaling functions*. The basic functions in orthogonal complements  $W_j := V_{j+1} \setminus V_j$  are referred to as *wavelet functions*:

$$\chi_k^j(x) = 2^{\frac{j}{2}} \chi(2^j x - k).$$

The spaces  $V_j$  and  $W_j$  have clear physical interpretation: If  $V_0$  is a space of functions measured with the most rough resolution  $L_0$ , then  $V_1$  has a twice better resolution  $L_0/2$ ;  $W_j$  represents the details to be lost by the coarse-graining from  $V_{j+1}$  to  $V_j$ .

Requirements of the orthonormality of basic functions and compactness of their support on  $[0, 2N - 1]$  for some  $N \in \mathbb{N}$  enables the iterative construction of the basic wavelets from the scaling equation:

$$\varphi(x) = \sqrt{2} \sum_k h_k \varphi(2x - k), \quad (11)$$

from where the basic wavelet functions are derived<sup>13</sup>:

$$\chi(x) = \sqrt{2} \sum_{k=0}^{2N-1} g_k \varphi(2x - k), \quad g_k = (-1)^k h_{2N+1-k}. \quad (12)$$

The simplest wavelet with compact support is the Haar wavelet, which is characterized by two basic functions  $\{\chi^i(x)\} = \{\varphi(x), \chi(x)\}$ , where the scaling function  $\varphi(x)$ <sup>17</sup> is the indicator function of the unit interval, and  $\chi(x)$  is the Haar wavelet:

$$\varphi(x) = \begin{cases} 1 : & 0 \leq x \leq 1, \\ 0 : & \text{otherwise} \end{cases}, \quad \chi(x) = \begin{cases} +1, & 0 \leq x < 1/2 \\ -1, & 1/2 \leq x < 1. \\ 0, & \text{otherwise} \end{cases} \quad (13)$$

The graphs of the both functions are shown in Fig. 1. The functions  $\varphi(x)$  and  $\chi(x)$ , except for the simplest Haar wavelet (13),  $N = 1$ , defined by a pair of coefficients  $h_0 = h_1 = \frac{1}{\sqrt{2}}$ , usually do not have any simple form, but are defined recursively<sup>13</sup>. Nevertheless, the existence of the exact relation (12), expressing the bases in the orthogonal complement spaces  $W_j$  in terms of the scaling function allows for fast and efficient numerical algorithms, when each space  $V_m$  is restricted to the space of functions piecewise constant on  $[2^m n, 2^m(n+1)]$ .

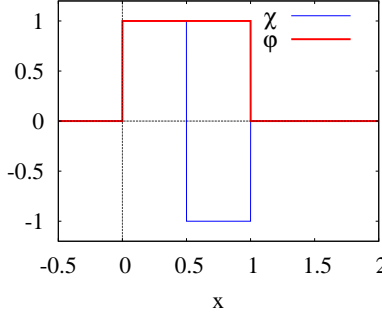


FIG. 1. The Haar wavelet  $\chi(x)$  and its scaling function  $\varphi(x)$

Provide the chain 1) is bounded from above by the best resolution space  $V_M$ , consisting for definiteness of  $2^M$  values

$$(c_0^M, \dots, c_{2^M-1}^M),$$

one can easily decompose this dataset into projections on

$$W_{M-1} \oplus \dots \oplus W_2 \oplus W_1 \oplus W_0 \oplus V_0$$

by applying a pair of filters  $(h, g)$ :

$$c_i^{j-1} = \sum_{k=0}^{2N-1} h_k c_{k+2i}^j, \quad d_i^{j-1} = \sum_{k=0}^{2N-1} g_k c_{k+2i}^j, \quad (14)$$

where  $c_i^j$  are coefficients of the projection on  $V_j$ ,  $d_i^j$  are coefficients of the projection on  $W_j$ , and periodic conditions are assumed in the discrete coordinate  $i$ .

### III. EUCLIDEAN SCALE-DEPENDENT QFT

In ordinary quantum field theory models the field functions are defined as the scalar product of the field state and the localization state (4). If we want to define the fields that depend not only on the localization point  $x$ , but also on the scale of measurement, and possibly on some parameters of observation, similarly to (4), we can define *scale-dependent fields*, or scale components of the field  $\phi$ , as:

$$\phi_{a\theta}(x) \equiv \langle x, a, \theta; \chi | \phi \rangle, \quad (15)$$

where  $\langle x, a, \theta; \chi |$  is the bra vector corresponding to localization of the measuring device around the point  $x$  with spatial resolution  $a$  and the orientation  $\theta \in SO(d)$ . The



mother wavelet  $\chi$  stands for the apparatus function of the device, or an aperture<sup>12</sup>. The scale-dependent functions (15) can be naturally defined in terms of continuous wavelet transform<sup>4,5</sup>.

To illustrate the method let us consider the theory of scalar field with  $\phi^4$  interaction, defined by the generating functional

$$Z[J] = \mathcal{N} \int \mathcal{D}\phi \exp \left( -S_E[\phi] + \int J(x)\phi(x)d^d x \right), \quad (16)$$

where

$$S_E[\phi] = \int_{\mathbb{R}^d} \left[ \frac{1}{2}(\nabla\phi)^2 + \frac{m^2}{2}\phi^2 + \frac{\lambda}{4!}\phi^4 \right] d^d x \quad (17)$$

is Euclidean action, and  $\mathcal{N}$  is a formal normalisation constant. The action (17) is an isotropic, translationally-invariant functional, similar to the Ginzburg-Landau free energy functional in the theory of phase transitions<sup>19</sup>. It coincides with the extrapolation of the energy of a classical interacting Ising spin system to a continuous limit in  $\mathbb{R}^{d20,21}$ , and describes many other physical systems. The connected Green functions of the theory with the Euclidean action (17), derived as functional derivatives of the generating functional,

$$G^{(n)}(x_1, \dots, x_n) = \frac{\delta^n \ln Z[J]}{\delta J(x_1) \dots \delta J(x_n)} \Big|_{J=0}, \quad (18)$$

suffer from UV divergences.

The straightforward way to get rid of UV divergence in Euclidean theory is to express the local field  $\phi(x)$  in terms of the inverse wavelet transform (9) and restrict the integration over all scale arguments to a limited range of scales  $\int_A^\infty \frac{da}{a} \dots$ , considering  $A$  as the finest resolution of observation. Unlike the momentum cutoff, the cutoff in scale argument does not produce any problems with the momentum conservation. This substitution provides a field theory model for scale-dependent fields  $\phi_a(x)$  determined by the generating functional

$$Z_W[J_a(x)] = \int \mathcal{D}\phi_a(x) \exp \left( -S_W[\phi_a(x)] + \int \phi_a(x)J_a(x) \frac{dad^d x}{C_\chi a} \right), \quad (19)$$

where we assume  $\chi$  to be an isotropic wavelet and drop the formal normalisation constant.

The action  $S_W[\phi_a(x)]$  is a result of wavelet transform of all fields in the original Euclidean action  $S_E[\phi(x)]$ . For the  $\phi^4$  field theory in  $\mathbb{R}^d$  we get

$$\begin{aligned} S_W[\phi_a(x)] = & \frac{1}{2} \int \phi_{a_1}(x_1) D(a_1, a_2, x_1 - x_2) \phi_{a_2}(x_2) \frac{da_1 d^d x_1}{C_\chi a_1} \frac{da_2 d^d x_2}{C_\chi a_2} \\ & + \frac{\lambda}{4!} \int V_{x_1, \dots, x_4}^{a_1, \dots, a_4} \phi_{a_1}(x_1) \dots \phi_{a_4}(x_4) \frac{da_1 d^d x_1}{C_\chi a_1} \frac{da_2 d^d x_2}{C_\chi a_2} \frac{da_3 d^d x_3}{C_\chi a_3} \frac{da_4 d^d x_4}{C_\chi a_4}, \end{aligned} \quad (20)$$

with  $D(a_1, a_2, x_1 - x_2)$  and  $V_{x_1, \dots, x_4}^{a_1, \dots, a_4}$  denoting the wavelet images of the inverse propagator and that of the interaction potential<sup>5</sup>.

All scale-dependent fields  $[\phi_a(x)]$  in Eq.(19) still interact with each other with the same coupling constant  $\lambda$ , but their interaction is now modulated by wavelet factor  $V_{x_1 x_2 x_3 x_4}^{a_1 a_2 a_3 a_4}$ , which is the Fourier transform of  $\prod_{i=1}^4 \tilde{\chi}(a_i k_i)$ .

Doing so, we have the following modification of the Feynman diagram technique<sup>4</sup>:

1. Each field  $\tilde{\phi}(k)$  is substituted by the scale component  $\tilde{\phi}(k) \rightarrow \tilde{\phi}_a(k) = \overline{\tilde{\chi}(ak)} \tilde{\phi}(k)$ .
2. Each integration in the momentum variable is accompanied by the corresponding scale integration

$$\frac{d^d k}{(2\pi)^d} \rightarrow \frac{d^d k}{(2\pi)^d} \frac{da}{a} \frac{1}{C_\chi}.$$

3. Each interaction vertex is substituted by its wavelet transform; for the  $N$ -th power interaction vertex, this gives multiplication by the factor  $\prod_{i=1}^N \tilde{\chi}(a_i k_i)$ .

According to these rules, the bare Green function in wavelet representation takes the form

$$G_0^{(2)}(a_1, a_2, p) = \frac{\tilde{\chi}(a_1 p) \tilde{\chi}(-a_2 p)}{p^2 + m^2}.$$

The finiteness of the loop integrals is provided by the following rule: *There should be no scales  $a_i$  in internal lines smaller than the minimal scale of all external lines*<sup>4,5</sup>. Therefore, the integration in  $a_i$  variables is performed from the minimal scale of all external lines up to infinity.

The generating functional  $Z_W[J_a(x)]$  is a partition function of a statistical model with a probability measure  $e^{-S_W[\phi_a(x)]} \mathcal{D}\phi_a(x)$  defining a probability of each field configuration  $\{\phi_a(x)\}_{a \in \mathbb{R}_+, x \in \mathbb{R}^d}$ . The Green functions

$$\langle \phi_{a_1}(x_1) \cdots \phi_{a_n}(x_n) \rangle_c = \left. \frac{\delta^n \ln Z_W[J_a]}{\delta J_{a_1}(x_1) \cdots \delta J_{a_n}(x_n)} \right|_{J=0},$$

are cumulants of the field  $\phi_a(x)$ .

If a given model with the 'action'  $S_W[\phi_a(x)]$  was derived from a local QFT model with polynomial interaction, then each internal line, connecting the  $i$ -th and the  $j$ -th vertices of a Feynman diagram, will contain two wavelet factors

$$\int_A^\infty |\tilde{\chi}(a_i p)|^2 \frac{da_i}{C_\chi a_i} \times \int_A^\infty |\tilde{\chi}(a_j p)|^2 \frac{da_j}{C_\chi a_j},$$

where  $p$  is the momentum of the line. This results in a squared wavelet cutoff factors  $f^2(Ap)$  in each diagram line, where

$$f(x) = \frac{1}{C_\chi} \int_x^\infty |\tilde{\chi}(a)|^2 \frac{da}{a} \quad (21)$$

for isotropic wavelets<sup>5</sup>. An evident normalization condition  $f(0) = 1$  corresponds to the common divergent theory in the infinite resolution limit  $A \rightarrow 0$ .

This factors  $f^2(Ap)$  present in each internal line suppress the UV divergences and make the scale-dependent QFT models with the generating functional (19) finite by construction. The renormalization group equations in the scale-dependent theory turn to be the logarithmic derivatives of the effective coupling constants, or effective parameters with respect to the logarithm of the observation scale  $-\frac{\partial}{\partial \ln A}$ <sup>7</sup>.

As usual in functional renormalization group technique<sup>22</sup>, we can introduce the effective action functional

$$\Gamma[\phi_a(x)] = -\ln Z_W[J_a(x)] + \int J_a(x) \phi_a(x) \frac{dad^d x}{C_\chi a}, \quad (22)$$

the functional derivatives of which are the vertex functions.

We can express it in a form of perturbation expansion:

$$\Gamma_{(A)}[\phi_a] = \Gamma_{(A)}^{(0)} + \sum_{n=1}^{\infty} \int \Gamma_{(A)}^{(n)}(a_1, b_1, \dots, a_n, b_n) \phi_{a_1}(b_1) \dots \phi_{a_n}(b_n) \frac{da_1 d^d b_1}{C_\chi a_1} \dots \frac{da_n d^d b_n}{C_\chi a_n}$$

The subscript  $(A)$  indicates the presence in the theory of minimal scale – the observation scale.

In analytical calculations it is convenient to use derivatives of the Gaussian as mother wavelets. The simplest is the first derivative of the Gaussian, which has Fourier transform

$$\tilde{\chi}_1(k) = -ik e^{-\frac{k^2}{2}}. \quad (23)$$

This results in the wavelet cutoff factor  $f_{\chi_1}(x) = e^{-x^2}$ . Considering the  $\phi^4$  model (20) in one-loop approximation

$$\Gamma^{(4)} = - \text{diagram 1} - \frac{3}{2} \text{diagram 2} \quad (24)$$

In four dimensions in the relativistic limit  $s^2 \gg 4m^2$  we get the following scaling equation for the coupling constant  $\lambda = \lambda^{eff}(A)$ :

$$\frac{\partial \lambda}{\partial \mu} = \frac{3\lambda^2}{16\pi^2} \frac{1 - e^{-\alpha^2}}{\alpha^2} e^{-\alpha^2}, \quad (25)$$

where  $\mu = -\ln A + const$ ,  $\alpha = As$ ,  $s = p_1 + p_2$ . The details of calculations are given in<sup>5,7</sup>.

In the limit of infinite resolution ( $A \rightarrow 0$ ) the scaling behaviour of the coupling constant (25) coincides with standard RG result. As it was shown in the recent paper<sup>23</sup>, the same is true for quantum electrodynamics: the asymptotic behaviour at small scales is independent on the particular type of the mother wavelet  $\chi$ , and coincides with the known RG behaviour. For finite scales  $A > 0$ , the type of the mother wavelet  $\chi$  certainly matters, because the scale components  $\phi_a(x)$  have been defined with respect to a given  $\chi$ .

## IV. SCALE-DEPENDENT QFT IN LIGHT-FRONT COORDINATES

### A. Geometric issues

Euclidean QFT models supplied with wavelet decomposition of the fields into scale components  $\phi_a(x)$ , as described in the previous section, provide finite Green functions for the fields defined on finite regions in  $\mathbb{R}^d$ , but these regions cannot be directly interpreted as spacetime regions. In the Minkowski space, in contrast, we cannot define a vicinity of a spacetime point  $x \in \mathbb{R}^{1,d-1}$  using a single mother wavelet. This is because the group  $SO(1,1)$  of Lorentz transformations of pseudo-Euclidean plane  $\mathbb{R}^{1,1}$  is not a simply-connected group, but includes four connected components

$$\begin{pmatrix} \cosh \eta & \sinh \eta \\ \sinh \eta & \cosh \eta \end{pmatrix}, \quad \begin{pmatrix} \cosh \eta & -\sinh \eta \\ \sinh \eta & -\cosh \eta \end{pmatrix}, \quad \begin{pmatrix} -\cosh \eta & \sinh \eta \\ -\sinh \eta & \cosh \eta \end{pmatrix}, \quad \begin{pmatrix} -\cosh \eta & -\sinh \eta \\ -\sinh \eta & -\cosh \eta \end{pmatrix},$$

parametrized by the Lorentz boost angle  $\tanh(\eta) = v/c$  – the *rapidity*. The light cone boundaries between these domains are unpassable for Lorentz boosts. Thus, according to<sup>24</sup>, instead of a single mother wavelet  $\chi(x)$ , the wavelet transform in pseudo-Euclidean plane requires *four* separate mother wavelets

$$\chi_j(x) = \int_{A_j} \frac{d\omega dk}{(2\pi)^2} \tilde{\chi}(k) e^{-i(\omega t - kx)}, \quad (26)$$

different from each other by their support in momentum space:

$$\begin{aligned}
A_1 : |\omega| > |k|, \omega > 0, & \quad A_2 : |\omega| > |k|, \omega < 0, \\
A_3 : |\omega| < |k|, \omega > 0, & \quad A_4 : |\omega| < |k|, \omega < 0.
\end{aligned} \tag{27}$$

Possible solution for tracing the propagation of a quantum particle from a finite spacetime region of its preparation to the finite region of its registration, in a way compatible with Lorentz invariance, is the use of light-front coordinates. *To some extent, what we want is a Lorentz-invariant theory with the spacetime regions being spanned by some wavelet basis in a way totally symmetric with respect to the space and the time variables.*

## B. Causality issues

We need a method to construct path integration over all causal paths from the finite-size region the field was prepared to the finite-size region of its registration. In standard quantum field theory approach, where the Feynman path of integration is understood as a continuous set of spacetime points, there is only one type of causality – the signal causality. Two events happening at two distinct spacetime points  $x$  and  $x'$ , separated by a space-like interval  $(x - x')^2 < 0$  cannot be causally connected. If two events  $A$  and  $B$  are separated by a time-like interval  $(x_A - x_B)^2 > 0$ , then the event  $A$  causally affects the event  $B$  if  $B$  is within the forward light cone of  $A$ , see Fig. 2. In reality, if we understand *an event* as a

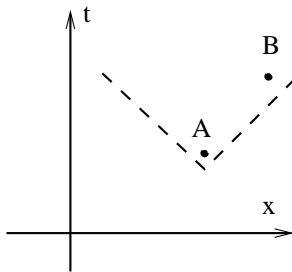


FIG. 2. Event  $A$  can causally affect event  $B$  only within the future-directed light cone.

change of the matter fields that *can be measured* (at least in principle); the events should be defined on finite-size regions, rather than points. This means, that beyond the signal causality, when two events  $A$  and  $B$  have an empty intersection  $A \cap B = \emptyset$ , there is another option:  $A \subset B$ , i.e,  $A$  is a part of  $B$ . Surprisingly, we are not very certain about what is the

vicinity of an event happening at a *point*  $x$  in the Minkowski space<sup>25</sup>. On one hand, it should be limited by the length of signal propagation during the event  $\Delta x \sim c\Delta t$ . On the other hand, it should be limited by quantum uncertainty of the event measurement  $\Delta p\Delta x \sim \frac{\hbar}{2}$ .

Since each of the events is associated with some measuring process, the latter case is easy to imagine in a *non-relativistic settings*. Let  $B$  be some measurement on a nucleon, and let  $A$  be some measurement on a constituent quark of that nucleon. The measurement on a quark (which is a part of the nucleon) is enabled by means of some preparation, or a measurement procedure, which have been performed on the nucleon. For instance, if the measured spin projection of nucleon to a given axis is  $+\frac{3}{2}$ , it is completely impossible for either of its constituents quarks have to have the projection of spin  $-\frac{1}{2}$  to the same axis. Thus, the knowledge of the state of the whole constrains possible states of its parts, i.e., the state of the whole is a *cause* for the states of its parts. Exactly this type of causality is manifested in the EPR-type experiments<sup>26</sup>, when measuring the spin of one particle we automatically get the value of its space-like separated remote partner's spin – tacitly exploiting the fact these two have been the parts of a common parent particle of spin zero.

It is rather easy to imagine such measurements in a non-relativistic case: the measurement domain of the part is just *inside* the measurement domain of the whole and the time difference between the measurements is regarded to be negligible. However, it is not easy to describe this situation in relativistic case. The reason is that the measurements performed at the same time for one observer, will be regarded as happening at different times for another observer. This also implies the problem of defining the *event vicinity* in Minkowski space. In Euclidean space a point  $x \in \mathbb{R}^d$  has a  $\epsilon$ -vicinity given by the Euclidian metrics:

$$V_\epsilon(x) = \{y \in \mathbb{R}^d | \sqrt{(x-y)^2} \leq \epsilon\}.$$

In Minkowski space, if we use the interval

$$s_{xy} = \sqrt{g_{\mu\nu}(x^\mu - y^\mu)(x^\nu - y^\nu)}, \quad g_{\mu\nu} = \text{diag}(1, -\mathbf{1}),$$

as a distance between  $x$  and  $y$ , it will be positively defined only within the future light-cone  $V^+(x)$  – the set of points which can be causally affected by  $x$ , and the past light-cone  $V^-(x)$  – the set of points that can causally affect  $x$ . Thus we can separately define the future

$\epsilon$ -vicinity and the past  $\epsilon$ -vicinity of  $x$ :

$$\begin{aligned} V_\epsilon^+(x) &= \{y \in \mathbb{R}^{1,3} | y^0 - x^0 \geq 0, 0 \leq (x - y)^2 \leq \epsilon^2\}, \\ V_\epsilon^-(x) &= \{y \in \mathbb{R}^{1,3} | y^0 - x^0 \leq 0, 0 \leq (x - y)^2 \leq \epsilon^2\}, \end{aligned} \quad (28)$$

with the only intersection  $V_\epsilon^+(x) \cap V_\epsilon^-(x) = x$ . The points belonging to the light cone are separated from  $x$  by zero (light-like) interval  $(x - y)^2 = 0$ . In this sense, any event on the light cone is indistinguishable from  $x$ , since in the coordinate system moving at the speed of light it is represented by the same point.

The vicinity  $V_\epsilon(x) := V_\epsilon^+(x) \cup V_\epsilon^-(x)$  is inconvenient for description of intersecting of events, one of which is the subset of the other. If we observe an event at  $P = (x^0, x^1)$  during the time interval  $\Delta t$  in a rest frame, our observation starts at  $P_- = (x^0 - \frac{\Delta t}{2}, x^1)$  and ends at  $P_+ = (x^0 + \frac{\Delta t}{2}, x^1)$ . This means the beginning of our observation potentially affects the forward light cone of  $P_-$ , thus the space-like separated events at the middle time  $x^0$  from  $(x^0, x^1 - \frac{c\Delta t}{2})$  to  $(x^0, x^1 + \frac{c\Delta t}{2})$  may be correlated. This suggests to chose the diamond  $D_{(x^0 - \frac{\Delta t}{2}, x^1)}^{(x^0 + \frac{\Delta t}{2}, x^1)}$  – that is the intersection of causal future of  $(x^0 - \frac{\Delta t}{2}, x^1)$  with the causal past of  $(x^0 + \frac{\Delta t}{2}, x^1)$  – as a causal  $\Delta t$ -vicinity of the event  $P = (x^0, x^1)$ . This set of vicinities is symbolically shown in Fig. 3.

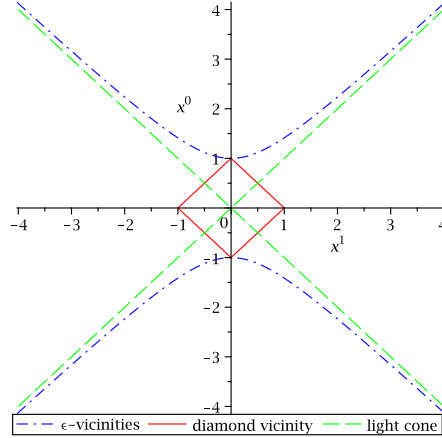


FIG. 3. Forward and backward vicinities of the event  $P = (0, 0)$  drawn in arbitrary units  $\epsilon = \frac{\Delta t}{2} = 1$ .  $V_\epsilon^\pm(P)$  are shown in dash-dot line. Dashed lines indicate the light cone  $x^1 = \pm x^0$ .

In general relativity theory a *causal path* connecting two spacetime events is a continuous curve  $x^\mu = x^\mu(s)$ , whose tangent vector is time-like or null everywhere  $\frac{dx^\mu}{ds} \frac{dx_\mu}{ds} \geq 0$ <sup>27</sup>. That is a causal path is a continuous set of spacetime points such that  $x^\mu(s) \prec x^\mu(s')$  if  $s < s'$ .

The concept of causal paths has been already extended in mathematics to discrete sequences of non-empty regions<sup>28,29</sup>:

$$A_1 \prec A_2 \prec \dots \prec A_n, \quad (29)$$

where  $A_i \prec A_j$  means that  $\forall x \in A_i, y \in A_j, x \prec y$ , in the sense that  $y$  is in the forward light cone of  $x$ . The region causality relations<sup>28</sup> are based on two binary partial order relations: the preceding  $\prec$  and the subset  $\subset$  relations.

**Definition 2** *A set of regions  $A, B, C, D, \dots \in \mathcal{Z}$  with two partial orders, such that:*

1. *The subset relation  $\subset$  is a partial order on the set of regions:*

$$A \subset B \text{ and } B \subset C \text{ implies } A \subset C,$$

$$A \subset A,$$

$$A \subset B \text{ and } B \subset A \text{ implies } A = B$$

2. *The partial order  $\subset$  has a minimum element  $\emptyset$ , which is contained in any region.*

3. *The partial order  $\subset$  has unions:*

$$A \subset A \cup B \text{ and } B \subset A \cup B,$$

$$\text{if } A \subset C \text{ and } B \subset C \text{ then } A \cup B \subset C$$

4. *The preceding relation  $\prec$  induces a strict partial order on the non-empty regions:*

$$A \prec B \text{ and } B \prec C \text{ implies } A \prec C,$$

$$A \not\prec A.$$

5.  $\forall A, B, C$ :

$$A \subset B \text{ and } B \prec C \text{ implies } A \prec C,$$

$$A \subset B \text{ and } C \prec B \text{ implies } C \prec A,$$

$$A \prec C \text{ and } B \prec C \text{ implies } A \cup B \prec C.$$

*is called a causal site.*

(Here we have simplified the definition 2.2 given in<sup>28</sup>, reducing some requirements, redundant for the present consideration.) Causal sites generalize the concepts of topology using the background of the *category theory*<sup>30</sup>. They were intended to describe quantum geometry in



the settings of quantum gravity, but they were not yet related to any measurement procedure aimed for the quantum fields defined on regions.

To adopt "the whole – the part" causality relations for an abstract measurement procedure and to define the integration over causal paths let us start from the consideration of non-relativistic case. In non-relativistic case, when the coordinate  $x$  takes its values in Euclidean space  $x \in \mathbb{R}^d$ , and the time  $t$  is a universal parameter, there exists a direct analogy of the scale-dependent fields  $\phi_a^i(b)$ . This is the Kadanoff blocking of the Ising ferromagnet<sup>31</sup>. The test function is then the indicator function of a unit  $d$ -dimensional cube. The  $n$ -point correlation functions

$$\langle \phi_{a_1}^{(i_1)}(b_1; t_1) \dots \phi_{a_n}^{(i_n)}(b_n; t_n) \rangle$$

are understood as the expectation of joint measurement of the spins, or the magnetic moments, of the blocks of different sizes  $a_1, \dots, a_n$ , centred at  $b_1, \dots, b_n$ , measured at different time instants  $t_1, \dots, t_n$ . The corresponding set of such events is graphically shown in Fig. 4. At coinciding time arguments the correlators can be evaluated using the ensemble averaging

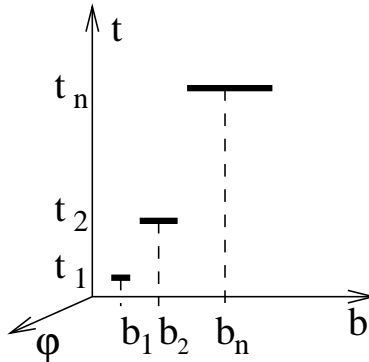


FIG. 4. Supports of the basic functions with time  $t$  treated as an independent parameter. Each event also extends in the direction of scale  $a$ , but this is not shown. The typical spatial widths of each measurements are  $a_1, a_2, a_3$ , respectively. The time duration of each measurement is assumed to be negligible.

common in statistical physics. The set of events, corresponding to the measurements of the field values  $\phi_{a_i}(b_i)$ , has no mutual intersection of events.

In other settings, when the measured fields do not depend on time – this happens in ergodic conditions when time averaging can be substituted by ensemble averaging, and only the spatial dependence is essential – there may be another relation between two measure-

ments. The latter is shown in Fig. 5. For instance, let the event  $A$  consist in measuring the

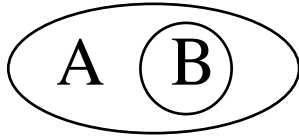


FIG. 5. Events in probability theory

fluctuations of certain field  $\phi$  over a sufficiently large spatial domain (let it be, for definiteness, the turbulent fluid velocity as described in<sup>32</sup>). Let the event  $B$  consist in measuring the velocity fluctuations in some smaller domain  $B$ , which is inside the domain  $A$ . The typical scales of fluctuations  $a$  in the smaller domain are also within the range of fluctuations in the larger one. In this case, the probability of a given field configuration in a smaller domain obeys the chain rule:

$$P(\phi_B) = \int P(\phi_B|\phi_A)P(\phi_A)\mathcal{D}\phi_A. \quad (30)$$

Thus, our measurement events turn to be the *events* in the common sense of an event algebra in probability theory<sup>8</sup>.

Any real physical measurement takes place in a certain spacetime domain of finite size. The idealization shown in Fig. 5, related to *space* only, obtained by an ensemble averaging, is impossible for instrumental measurement, because the limit  $\Delta t \rightarrow 0$  cannot be achieved. Hence, we face a topological question: What sequences of spacetime regions can comprise a path in the space of measurements, compatible with both the relativistic invariance and the event algebra of the probability theory?

The Fig. 5, which totally ignores the finite time of measurement, but calculates the probability of the measurement result on a smaller region ( $B$ ) *conditionally* to the state of fields on its parent region ( $A$ ), is too strong exaggeration for the quantum world. Each quantum measurement is associated with a certain physical interaction. The lower is the energy of this interaction, the higher is the uncertainty in the coordinate and the longer is time of measurement. To measure the state of an electron in atom, we first localize the atom by certain *soft measurement* of typical size  $L$ , and only then perform the measurement on the electron itself. The time and the space uncertainty in the electron position may be kept deeply within the atom position  $l \ll L$ , see Fig. 6.

Even if the atom localization starts with a point interaction at  $(0,0)$  and continues for

the time  $2T$ , the measurement can be affected by the information from the whole spacetime diamond of size  $2T$  shown in Fig. 6. Thus the shape of any spacetime region that pretends

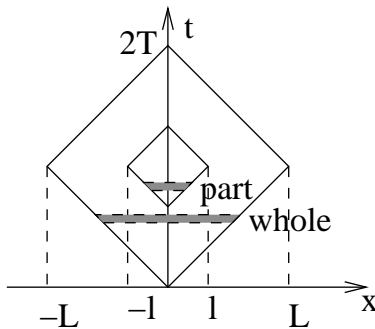


FIG. 6. Sequential measurements of an electron inside an atom performed in the rest frame of the atom

to be a measurement event is restricted by the causal diamond of the measuring setup. The distance between the beginning of the atom preparation and the measurement performed on the electron is given in the rest frame of the atom. However, the time difference between the different events depends on the choice of Lorentz frame.

There are at least two ways to describe such hierarchic measurements. First, if the initial configuration of the measured system have been prepared of some equal-time hypersurface  $\Sigma_{t_0}$  at the time instant  $t_0$ , we can slice the Minkowski spacetime into an ordered sequence of hypersurfaces  $\Sigma_{t_0} \prec \Sigma_{t_1} \prec \dots \Sigma_{t_n}$ , such that  $t_0 < t_1 < \dots < t_n$ . This instant-type description is based on a partially-ordered set:  $B \subset A \subset \Sigma_t$  implies that  $A$  is a cause of  $B$ , but if the sets  $A \cap B = \emptyset$  are separated by a space-like interval they cannot be causally ordered. To build a *continuous* trajectory of such sets  $A_1 \prec A_2 \prec \dots$  the distance between sequential sets ought to vanish:

$$A_1 \prec A_2, \lim_{t_2-t_1 \rightarrow 0} d(A_1, A_2) = 0, \quad \text{where } d(A_1, A_2) := \sqrt{\min |(t_1 - t_2)^2 - (x_1 - x_2)^2|}. \quad (31)$$

The quantization scheme based on the ordering (31) is quite straightforward: the time-slices  $\Sigma_t$  are ordered according to the time argument; the field operators corresponding to different domains of the same slice are ordered according to the rule "the bigger domain acts on vacuum first"<sup>5</sup>. However since the size of the time lag  $\Delta t = t_n - t_{n-1}$  has no relations to the spacial size of the domains  $A_i$  this procedure does not manifest Lorentz covariance<sup>1</sup>.

Second, to construct a Lorentz-invariant description, i.e., to be able to calculate the quantum transition amplitudes independently of the Lorentz frame, we can change the

coordinates to the light-front form  $(x^+, x^-, x^2, x^3)$ :

$$\begin{pmatrix} x^+ \\ x^- \end{pmatrix} = \frac{1}{\sqrt{2}} \begin{pmatrix} 1 & 1 \\ 1 & -1 \end{pmatrix} \begin{pmatrix} x^0 \\ x^1 \end{pmatrix}. \quad (32)$$

This implies a metrics

$$g_{\alpha\beta} = \begin{pmatrix} 0 & 1 & 0 & 0 \\ 1 & 0 & 0 & 0 \\ 0 & 0 & -1 & 0 \\ 0 & 0 & 0 & -1 \end{pmatrix},$$

so that  $x_+ = x^-$ ,  $x_- = x^+$ ,  $x_{2,3} = -x^{2,3}$ ,  $x^2 = (x^0)^2 - (x^1)^2 - (x^2)^2 - (x^3)^2 = 2x^+x^- - (x^\perp)^2$ . The factor  $\sqrt{2}$  in the definition (32) corresponds to the Kogut and Soper convention<sup>9</sup>, and can be lifted with appropriate rescaling of  $g_{\alpha\beta}$ .

To make our causal description totally symmetric with respect to the space ( $x^1 \equiv x$ ) and the time ( $x^0 \equiv t$ ) coordinates, we can consider the following construction. Let the observer be capable of observing a region of typical time span  $2T$ , and hence the maximal spatial size  $2cT$ , and let his best resolution be  $\Delta t = T$ , i.e., the observer is capable of discriminating the observed object to be in the left, or right part of the observed domain – in the space or in the time direction, respectively. The standard (signal) ordering implies a partial order on

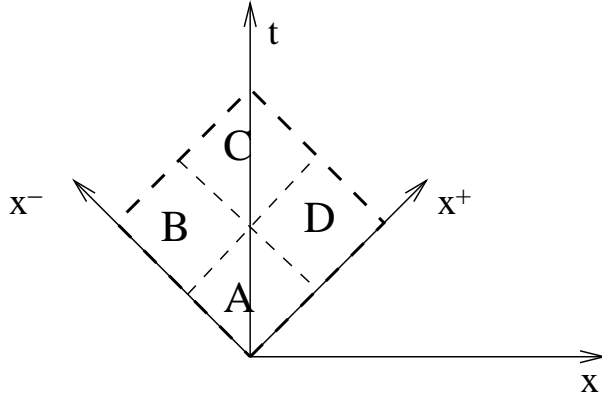


FIG. 7. Binary discriminated region  $\Theta$  in Minkowski plane. If the system was initially prepared in the domain  $A$  and finally registered in the domain  $C$ , there are 3 possible trajectories between these regions:  $(ABC)$ ,  $(ADC)$ ,  $(AC)$ . The light-front coordinates  $x^+ = \frac{t+x}{\sqrt{2}}$ ,  $x^- = \frac{t-x}{\sqrt{2}}$  enable symmetric partition of the spacetime region  $\Theta$ .

the set  $\Theta = A \cup B \cup C \cup D$ , see Fig. 7:

$$A \prec B \prec C, A \prec D \prec C.$$

The regions,  $B$  and  $D$ , being separated by a space-like interval, are not causally ordered. In the picture shown in Fig. 7, the  $B$  and  $D$  are simultaneous, but in other Lorentz frames it may be either  $B \prec D$ , or  $D \prec B$ .

To define paths on the set of regions independently of the Lorentz frame we need a set of test functions, which characterise each event region. It is convenient to define such basic functions in terms of the light-front variables. Let us consider a wavepacket of constant shape  $\phi(\cdot)$  moving in the positive direction of the  $x$  axis at the speed of light ( $c = 1$ ):  $\phi = \phi(t - x)$ . This wavepacket can scan the spacetime points in the vicinity of the light-front  $t \approx x$ , and the only way to discriminate the records of such events is to use the complementary variable  $x^+ = \frac{t+x}{\sqrt{2}}$  as a *time coordinate*. Launching similar packets from different "space locations"  $x^-$  one can scan different spacetime regions. Perhaps, by voluntary choice of the right-moving direction  $x^-$ , we have violated the symmetry between the left-moving and right-moving waves, but in this settings we can use the complementary variable  $x^+$  as the time coordinate for the construction of the Feynman functional integration. This change of variables is advantageous in collider experiments, with their preferable direction of the beam of relativistic particles<sup>33,34</sup>.

In the light-front variables  $(x^-, x^+)$  the diamond, shown in Fig. 7, turns to be a rectangle, the points of which can be ordered along the "time" direction  $x^+$ . Having this done, we can construct the equal- $x^+$  commutation relations for the fields at different  $x^-$ -locations.

In the case of the scale-dependent theory, when the causal trajectory is understood as a sequence of possible measurements performed on different spacetime regions, the operators defined on spacetime regions should first be ordered with respect to the subset relation ( $\subset$ ), and only then according to the signal causality relation ( $\prec$ ). For instance, if we observe a quantum system described by a single coordinate  $q = q(t)$  during the time interval  $t \in [0, T)$  with the best time resolution  $\Delta t = \frac{T}{4}$ , the operators should be ordered as shown in Fig. 8. First, we locate the system, or a particle, at the beginning of the trajectory by registering its existence on intervals  $1 \rightarrow 2 \rightarrow 3$ , then the movement  $3 \rightarrow 4$  is registered. The transport of the system to the next time cell '6' is registered in two steps: first the particle is located in the right half-interval '5', and then located in the left quarter '6'. The physical fields characterising such system  $q_{[0,T)}, q_{[0,T/2)}, q_{[T/2,T)}, \dots$  can be measured using the waves of different frequencies.

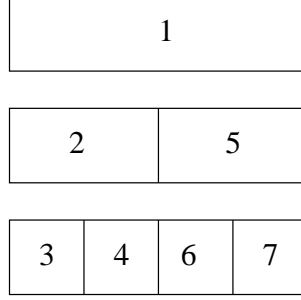


FIG. 8. Ordering of hierarchical events on a one-dimensional interval.

### C. Path integration over the event regions

To illustrate the path integration over the fields that depend on regions, rather than points let us consider a simple quantum system with a single degree of freedom, say a harmonic oscillator. In quantum mechanics the amplitude of a quantum transition of such system from initial quantum state  $|Q\rangle$  at time  $t = 0$  to the final quantum state  $|Q'\rangle$  at time  $t = T > 0$  is given by the equation

$$\langle Q'|Q\rangle \propto \int \mathcal{D}q e^{\frac{i}{\hbar} \int_0^T L[q(t)]dt}, \quad (33)$$

where  $L[q]$  is the Lagrangian of the system, and  $\mathcal{D}q$  is the Feynman's measure.

To calculate the transition amplitude (33) the time interval  $[0, T]$  should be divided into small time-slices  $0 < t_1 < \dots t_n < T$ , so that in infinitesimal limit ( $n \rightarrow \infty$ )

$$\mathcal{D}q = \prod_{i=1}^n dq(t_i), \quad \max_i (t_i - t_{i-1}) \rightarrow 0.$$

Since  $q(t)$  can be considered as a quantum field on the one-dimensional interval  $[0, T]$ , we can introduce the scale-dependent fields, defined on finite-size regions, using wavelet transform. For the compact manifold  $[0, T]$  it is natural to use the *discrete wavelet transform* using compactly supported wavelets<sup>13,17</sup>. In case of the discrete wavelet transform<sup>13</sup> the integrals over the scale variable  $\frac{da}{a}$  become discrete sums  $\sum_m d_n^m \chi_{mn}(t)$ , where

$$\chi_{mn}(t) := a_0^{-\frac{m}{2}} \chi(a_0^{-m}t - nb_0), \quad (34)$$

with  $a_0 = 2$  being the common choice. The discrete set of wavelet coefficients is given by

$$d_n^m := \int_0^T a_0^{-\frac{m}{2}} \bar{\chi}(a_0^{-m}t - nb_0) q(t)dt \equiv \langle \chi_{mn}|q\rangle. \quad (35)$$

For simplicity let us consider the field  $q(t)$  on the time interval  $[0, T]$  written as a sequence of  $2^N$  values  $q_0, q_1, \dots, q_{2^N-1}$ , at sequential time instants, where  $q_0 = q(0)$  and  $q_{2^N-1} = q(T)$ . Using the discrete wavelet transform, with the simplest orthogonal wavelet – the Haar wavelet (13) – we have the mapping

$$q_0, \dots, q_{2^N-1} \rightarrow d_0^1 \dots d_{2^{N-1}-1}^1, d_0^2 \dots d_{2^{N-2}-1}^2, \dots d_0^N c_0^N,$$

given by the iterative procedure of the fast wavelet transform algorithm

$$c_k^{j+1} = \frac{c_{2k}^j + c_{2k+1}^j}{\sqrt{2}}, \quad d_k^{j+1} = \frac{c_{2k}^j - c_{2k+1}^j}{\sqrt{2}}, \quad j \in \mathbb{N} \quad (36)$$

with the initial data  $q_k \equiv c_k^0$ . The algorithm (36) conserves the number of independent degrees of freedom and is linearly invertible.

In the toy model of  $N = 2$  we get a mapping  $q_0, q_1, q_2, q_3 \rightarrow d_0^1, d_1^1, d_0^2, c_0^2$ , with a two-scale decomposition of the initial data:

$$\begin{aligned} d_0^1 &= \frac{q_0 - q_1}{\sqrt{2}}, & d_1^1 &= \frac{q_2 - q_3}{\sqrt{2}}, \\ d_0^2 &= \frac{q_0 + q_1 - q_2 - q_3}{2}, & c_0^2 &= \frac{q_0 + q_1 + q_2 + q_3}{2}. \end{aligned}$$

The last coefficient  $c_0^2$  is merely the mean value of the field  $q$ , which can be eliminated in continual limit  $N \rightarrow \infty$ . The wavelet coefficient  $d_0^2$  is responsible for the global dynamics of the field  $q$  on the whole time interval  $[0, T]$ . The coefficients  $d_0^1$  and  $d_1^1$  are responsible for the dynamics of the field  $q$  on the left and the right half-intervals, respectively. Thus, instead of integration over  $q_1$  and  $q_2$  (at fixed  $q_0, q_3$ ), we can integrate over  $d_0^1, d_1^1$ , keeping fixed the remaining wavelet coefficients. If the coefficients  $d_n^m$  are *operators*, they can be naturally ordered according to the tree shown in Fig. 8.

Now we can consider similar hierarchic ordering in the partition of the square  $[0, T] \otimes [0, T]$  in the  $(x^+, x^-)$  plane, considering  $x^+$  as the time and  $x^-$  as the space variable. In two dimensions to store the information written in each 4 points of the  $j$  hierarchy level

$$(c_{2k,2m}^j, c_{2k+1,2m}^j, c_{2k,2m+1}^j, c_{2k+1,2m+1}^j)$$

we need 4 basic functions:

$$\begin{aligned} \varphi(x^+) \varphi(x^-) & \quad \chi(x^+) \varphi(x^-) \\ \varphi(x^+) \chi(x^-) & \quad \chi(x^+) \chi(x^-), \end{aligned} \quad (37)$$

where  $\chi(\cdot)$  is the basic wavelet and  $\varphi(\cdot)$  is the scaling function. In our case  $\chi$  is the Haar wavelet, and  $\varphi$  is the indicator function of the unit interval, see Fig. 1.

Thus at each next hierarchy level  $(j + 1)$  we have 4 wavelet coefficients

$$\begin{aligned} c_{k,m}^{j+1} &= \frac{c_{2k,2m}^j + c_{2k,2m+1}^j + c_{2k+1,2m}^j + c_{2k+1,2m+1}^j}{2}, \\ d_{k,m}^{(1),j+1} &= \frac{c_{2k,2m}^j - c_{2k,2m+1}^j + c_{2k+1,2m}^j - c_{2k+1,2m+1}^j}{2}, \\ d_{k,m}^{(2),j+1} &= \frac{c_{2k,2m}^j + c_{2k,2m+1}^j - c_{2k+1,2m}^j - c_{2k+1,2m+1}^j}{2}, \\ d_{k,m}^{(3),j+1} &= \frac{c_{2k,2m}^j - c_{2k,2m+1}^j - c_{2k+1,2m}^j + c_{2k+1,2m+1}^j}{2}. \end{aligned} \tag{38}$$

The first coefficient  $c$  is proportional to the mean values of the field in the 4 cells it inherits.  $d^{(1)}$  is sensitive to the movement in the  $x^-$  direction,  $d^{(2)}$  is sensitive to the movement in  $x^+$  direction, and  $d^{(3)}$  is sensitive to time-like movement. So, this hierarchic description in terms of the light cone variables  $x^+$  and  $x^-$  is absolutely symmetric with respect to the "time"  $x^+$  and the "space"  $x^-$ . The movements are allowed in all three directions. The change to the next cell is performed by increasing the hierarchy level  $j \rightarrow j + 1$ , followed by appropriate localization of the subcell.

To exploit this method we can start with a  $(1 + 1)$ -dimensional scalar field theory with  $\phi^4$ -interaction, written in light-front coordinates, see, e.g.<sup>35</sup>. Considering the square domain  $D = [0, T] \otimes [0, T]$  in the  $(x^+, x^-)$  plane, and the action functional

$$S[\phi] = \int_0^T dx^+ \int_0^T dx^- \left[ \frac{\partial \phi}{\partial x^+} \frac{\partial \phi}{\partial x^-} - \frac{m^2}{2} \phi^2 - \frac{\lambda}{4!} \phi^4 \right], \tag{39}$$

originated from the standard Lagrangian of  $\phi^4$  theory, We can formally decompose the field  $\phi(x^+, x^-)$  into the scale components

$$\phi(x^+, x^-) = \sum d_{j,k_1,k_2}^{m_1,m_2} \chi_{j,k_1}^{m_1}(x^+) \chi_{j,k_2}^{m_2}(x^-), \tag{40}$$

where the upper indices  $m_1, m_2 \in \{h, g\}$  designate the type of basic function:  $\chi^h \equiv \varphi$ ,  $\chi^g \equiv \chi$ . Similar decomposition can be written for a full four-dimensional case of  $\phi(x^+, x^-, \mathbf{x}_\perp)$ . The advantage of the orthogonal wavelet bases is that supports of these functions do not have partial intersection: they are either disjoint, or one within another. This agrees with the space-time picture of quantum measurements, which can be performed either in separate space-time regions, or the state of a subregion is inferred from the measurement on the whole region.



Using the bases of orthogonal wavelets in  $L^2(\mathbb{R})$  the summation over all basic functions provides the partition of a unity. Due to this property, the mass term

$$\frac{m^2}{2} \int \phi^2 dx^+ dx^-$$

turns into a sum of modulus squared wavelet coefficients

$$\frac{m^2}{2} \sum |d_{j,k_1 k_2}^{m_1 m_2}|^2.$$

Similarly, for the generative part

$$\int J(x) \phi(x) dx^+ dx^- \rightarrow \sum J_{j,k_1,k_2}^{m_1,m_2} d_{j,k_1 k_2}^{m_1 m_2}.$$

The other terms in the action (39) are expressed in terms of the so-called *wavelet connection coefficients*. The kinetic term is expressed as a product of two identical coefficients in  $x^+$  and  $x^-$  coordinates:

$$\begin{aligned} \int \frac{\partial \phi}{\partial x^+} \frac{\partial \phi}{\partial x^-} dx^+ dx^- &= - \int \phi \frac{\partial^2}{\partial x^+ \partial x^-} \phi dx^+ dx^- \\ &= - \int d_{j',k'_1,k'_2}^{m'_1,m'_2} \chi_{j',k'_1}^{m'_1}(x^+) \chi_{j',k'_2}^{m'_2}(x^-) d_{j,k_1,k_2}^{m_1,m_2} \frac{\partial \chi_{j,k_1}^{m_1}(x^+)}{\partial x^+} \frac{\partial \chi_{j,k_2}^{m_2}(x^-)}{\partial x^-} dx^+ dx^- \\ &= - d_{j',k'_1,k'_2}^{m'_1,m'_2} d_{j,k_1,k_2}^{m_1,m_2} \Omega_{j',k_1-k'_1}^{m'_1,m_1} \Omega_{j,k_2-k'_2}^{m'_2,m_2} \end{aligned}$$

These connection coefficients  $\Omega_{j,k-k'}^{m',m} := \int dx \chi_{j,k'}^{m'}(x) \frac{\partial \chi_{j,k}^m(x)}{\partial x}$  are presented in<sup>1,36,37</sup>. Thus the whole generating functional can be written as the integral over all wavelet coefficients spanning the domain  $[0, T] \otimes [0, T]$  in the  $(x^+, x^-)$  plane:

$$Z[J] = \int \mathcal{D} d_{j,k_1,k_2,\dots}^{m_1,m_2,\dots} e^{\frac{i}{\hbar} S[d_{j,k_1,k_2,\dots}^{m_1,m_2,\dots}] + i d_{j,k_1,k_2,\dots}^{m_1,m_2,\dots} J_{j,k_1,k_2,\dots}^{m_1,m_2,\dots}} \quad (41)$$

Here the functional integration symbol  $\mathcal{D}$  means the product of differentials of all wavelet coefficients. To make the generation functional (41) and corresponding Green functions finite, the set of wavelet coefficients should be restricted by certain best resolution scale. The restriction of the number of scales is a usual thing in numerical wavelet transform. In case of quantum field theory this is a kind of lattice regularization<sup>38</sup>.

The wavelet coefficients  $d_{j,k_1,k_2}^{m_1,m_2}; m_1, m_2 \in \{h, g\}$  represent 4 possible types of fields supported by finite-size regions in  $(x^+, x^-)$  plane. Similar construction for any field  $f$  can be presented in terms of continuous wavelet transform written in light-front coordinates. Since the continuous wavelet transform in Minkowski space is defined separately in 4 domains (27)

$$A_1 : k^+ > 0, k^- > 0, \quad A_2 : k^+ < 0, k^- > 0, \quad A_3 : k^+ > 0, k^- < 0, \quad A_4 : k^+ < 0, k^- < 0,$$

we have a set of 4 different wavelet coefficients

$$W_{ab\eta\phi}^i = \int_{A_i} e^{ik_-b_+ + ik_+b_- - i\mathbf{k}_\perp \mathbf{b}_\perp} \tilde{f}(k_-, k_+, \mathbf{k}_\perp) \bar{\chi}(ae^\eta k_-, ae^{-\eta} k_+, aR^{-1}(\phi)\mathbf{k}_\perp) \frac{dk_+ dk_- d^2\mathbf{k}_\perp}{(2\pi)^4}, \quad (42)$$

where  $\eta$  is the boost angle, and  $R(\phi)$  is rotation matrix<sup>6,39</sup>. However, for technical reasons analytic calculations of loop integrals are easier in Euclidean version of the scale-dependent theory described in *Section III*.

## V. CONCLUSION

In present paper we have considered the application of wavelet transform to the quantum field theory models written in light front variables. Our research have been inspired by a recent paper<sup>1</sup>, where the author used the  $x^+$  variable as 'time, for time-ordering only, but applied wavelet transform to the remaining 'spatial' coordinates  $(x^-, \mathbf{x}^\perp)$  to resolve details of different scales. This approach, although being favourable in high-energy physics settings with prescribed beam direction, introduces an asymmetry between  $x^+$  and  $x^-$ , and hence an asymmetry between the forward and backward motion along the  $x$ -axis.

We have shown that quantum field theory models can be written in light-front variables in a way totally symmetric with respect to  $x^+$  and  $x^-$ . Feynman path integral in our approach turns to be the sum over all possible sequences of *events* between the initial and the final space-time region supplied with operator-valued measure, which describes the quantum field that can be potentially measured on this region. The representation of this measure in terms of wavelet transform is symmetric with respect to  $x^+$  and  $x^-$  variables. Its value is limited by the scale parameter – the best resolution of measurement, – i.e. the minimal size of space-time domain the measurement can be carried on. This leads to quantum field theory models finite by construction.

In our approach the causal ordering of events takes place not only in time ( $x^+$  or  $x^-$ ), as usual, but also by inclusion: the event  $\phi_B$  is constrained by event  $\phi_A$  if  $B \subset A$ , where  $A$  and  $B$  are two space-time regions. As a matter of fact, our approach generalises the notion of space-time event happening at  $P \in \mathbb{R}^{1,3}$  to more general definition adopted in probability theory.

Starting from the flat Minkowski space and considering a simple toy model the authors understand that a consistent account of path integration over finite-size regions may be given

only in terms of quantum gravity theory, where different tree-like structures, similar to our construction of discrete wavelet transform, are already in use, say in terms of the AdS/CFT correspondence<sup>40</sup>. This will be the subject of future work.

## STATEMENTS AND DECLARATIONS

The authors have no competing interests. All authors have been paid from budget - no funding acknowledgement is required.

## ACKNOWLEDGEMENT

The authors are thankful to Profs. J.-P. Gazeau, M.Hnatich, S.Mikhailov, M.Perel, and W.N.Polyzou for useful comments and references.

## REFERENCES

- <sup>1</sup>W. Polyzou, “Wavelet representation of light-front quantum field theory,” *Phys. Rev. D* **101**, 096004 (2020).
- <sup>2</sup>P. Dirac, “The Lagrangian in quantum mechanics,” *Physikalische Zeitschrift der Sowietunion* **3**, 64–72 (1933).
- <sup>3</sup>R. P. Feynman, “Space-time approach to quantum electrodynamics,” *Phys. Rev.* **76**, 769–789 (1949).
- <sup>4</sup>M. V. Altaisky, “Wavelet based regularization for Euclidean field theory,” *IOP Conf. Ser.* **173**, 893–897 (2003).
- <sup>5</sup>M. V. Altaisky, “Quantum field theory without divergences,” *Phys. Rev. D* **81**, 125003 (2010).
- <sup>6</sup>M. V. Altaisky and N. E. Kaputkina, “Continuous wavelet transform in quantum field theory,” *Phys. Rev. D* **88**, 025015 (2013).
- <sup>7</sup>M. V. Altaisky, “Unifying renormalization group and the continuous wavelet transform,” *Phys. Rev. D* **93**, 105043 (2016).
- <sup>8</sup>A. Kolmogorov, *Foundations of the Theory of Probability*, 2nd ed. (Dover Publications, 2018).

- <sup>9</sup>J. Kogut and D. Soper, “Quantum electrodynamics in the infinite-momentum frame,” *Phys. Rev. D* **1**, 2901–2914 (1970).
- <sup>10</sup>P. Goupillaud, A. Grossmann, and J. Morlet, “Cycle-octave and related transforms in seismic signal analysis,” *Geoexploration* **23**, 85–102 (1984).
- <sup>11</sup>C. M. Handy and R. Murenzi, “Moment-wavelet quantization: a first principles analysis of quantum mechanics through continuous wavelet transform theory,” *Phys. Lett. A* **248**, 7–15 (1998).
- <sup>12</sup>E. Freysz, B. Pouligny, F. Argoul, and A. Arneodo, “Optical wavelet transform of fractal aggregates,” *Phys. Rev. Lett.* **64**, 745–748 (1990).
- <sup>13</sup>I. Daubechies, “Orthonormal bases of compactly supported wavelets,” *Comm. Pure. Apl. Math.* **41**, 909–996 (1988).
- <sup>14</sup>A. L. Carey, “Square-integrable representations of non-unimodular groups,” *Bull. Austr. Math. Soc.* **15**, 1–12 (1976).
- <sup>15</sup>M. Duflo and C. C. Moore, “On regular representations of nonunimodular locally compact group,” *J. Func. Anal.* **21**, 209–243 (1976).
- <sup>16</sup>G. Beylkin, R. Coifman, and V. Rokhlin, “Fast wavelet transforms and numerical algorithms. I,” *Comm. Pure. Apl. Math.* **44**, 141–183 (1991).
- <sup>17</sup>I. Daubechies, *Ten lectures on wavelets* (S.I.A.M., Philadelphie, 1992).
- <sup>18</sup>S. Mallat, “A theory for multiresolution signal decomposition: wavelet transform,” (1986), preprint GRASP Lab. Dept. of Computer an Information Science, Univ. of Pensilvania.
- <sup>19</sup>V. Ginzburg and L. Landau, “On the theory of superconductivity,” *Zh. Eksp. Teor. Fiz.* **20**, 1064 (1950).
- <sup>20</sup>K. G. Wilson and J. Kogut, “The renormalization group and the  $\epsilon$  expansion,” *Physics Reports* **12**, 75–199 (1974).
- <sup>21</sup>J. Berges, N. Tetradis, and C. Wetterich, “Non-perturbative renormalization flow in quantum field theory and statistical physics,” *Physics reports* **363**, 223–386 (2002).
- <sup>22</sup>C. Wetterich, “Exact evolution equation for the effective potential,” *Phys. Lett. B* **301**, 90 – 94 (1993).
- <sup>23</sup>M. V. Altaisky and R. Raj, “Wavelet regularization of Euclidean QED,” *Phys. Rev. D* **102**, 125021 (2020).
- <sup>24</sup>E. Gorodnitskiy and M. Perel, “Integral representations of solutions of the wave equation based on relativistic wavelets,” *J. Math. Phys.* **45**, 385203 (2012).

- <sup>25</sup>D. Blokhintsev, *Space and Time in Microworld* (Springer, 1973).
- <sup>26</sup>A. Einstein, B. Podolsky, and N. Rosen, “Can quantum-mechanical description of physical reality be considered complete?” *Phys. Rev.* **47**, 777–780 (1935).
- <sup>27</sup>E. Witten, “Light rays, singularities, and all that,” *Rev. Mod. Phys.* **92**, 045004 (2020).
- <sup>28</sup>J. D. Christensen and L. Crane, “Causal sites as quantum geometry,” *J. Math. Phys.* **46**, 122502 (2005).
- <sup>29</sup>E. Dable-Heath, C. J. Fewster, K. Rejzner, and N. Woods, “Algebraic classical and quantum field theory on causal sets,” *Phys. Rev. D* **101**, 065013 (2020).
- <sup>30</sup>S. Mac Lane and I. Moerdijk, *Sheaves in Geometry and Logic, a First Introduction to Topos Theory* (Springer-Verlag, 1992).
- <sup>31</sup>L. P. Kadanoff, “Scaling laws for Ising models near  $T_c$ ,” *Physics* **2**, 263–272 (1966).
- <sup>32</sup>M. V. Altaisky, M. Hnatich, and N. E. Kaputkina, “Renormalization of viscosity in wavelet-based model of turbulence,” *Phys. Rev. E* **98**, 033116 (2018).
- <sup>33</sup>G. Chen, Y. Li, K. Tuchin, and J. P. Vary, “Heavy quarkonia production at energies available at the CERN Large Hadron Collider and future electron-ion colliding facilities using basis light-front quantization wave functions,” *Phys. Rev. C* **100**, 025208 (2019).
- <sup>34</sup>J. Berges, M. P. Heller, A. Mazeliauskas, and R. Venugopalan, “QCD thermalization: Ab initio approaches and interdisciplinary connections,” *Rev. Mod. Phys.* **93**, 035003 (2021).
- <sup>35</sup>S. S. Chabysheva and J. R. Hiller, “Transitioning from equal-time to light-front quantization in  $\phi_2^4$  theory,” *Phys. Rev. D* **102**, 116010 (2020).
- <sup>36</sup>J. M. Restrepo and G. K. Leaf, “Inner product computations using periodized Daubechies wavelets,” *International Journal for Numerical Methods in Engineering* **40**, 3557–3578 (1997).
- <sup>37</sup>F. Bulut, “An alternative approach to compute wavelet connection coefficients,” *Applied Mathematics Letters* **53**, 1–9 (2016).
- <sup>38</sup>G. Battle, *Wavelets and renormalization group* (World Scientific, 1999).
- <sup>39</sup>M. Altaisky and N. Kaputkina, “On the wavelet decomposition in light cone variables,” *Russian Physics Journal* **55**, 1177–1182 (2013).
- <sup>40</sup>M. Miyaji, T. Takayanagi, and K. Watanabe, “From path integrals to tensor networks for the AdS/CFT correspondence,” *Phys. Rev. D* **95**, 066004 (2017).